sustainability

MDPI

Article

Hazardous Elements in Sediments Detected in Former Decommissioned Coal Mining Areas in Colombia: A Need for Environmental Recovery

Marcos L. S. Oliveira [1,2,*], Gabriela Oliveira Valença [2], Diana Pinto [1], Leila Dal Moro [3], Brian William Bodah [3,4,5], Giana de Vargas Mores [3], Julian Grub [6], Bashir Adelodun [7,8] and Alcindo Neckel [3,*]

1 Department of Civil and Environmental Engineering, Universidad de la Costa, CUC, Calle 58 # 55–66, Barranquilla 080002, Colombia; dpinto3@cuc.edu.co
2 Department of Sanitary and Environmental Engineering, Federal University of Santa Catarina, UFSC, Campus Universitário Trindade, Florianópolis 87504-200, Brazil; gabriela.ovalenca@gmail.com
3 ATITUS Educação, Passo Fundo 99070-220, Brazil; leila.moro@atitus.edu.br (L.D.M.); bbodah@yvcc.edu (B.W.B.); giana.mores@atitus.edu.br (G.d.V.M.)
4 Thaines and Bodah Center for Education and Development, 840 South Meadowlark Lane, Othello, WA 99344, USA
5 Workforce Education & Applied Baccalaureate Programs, Yakima Valley College, South 16th Avenue & Nob Hill Boulevard, Yakima, WA 98902, USA
6 Department of Architecture and Urbanism, University of Vale do Rio dos Sinos, UNISINOS, São Leopoldo 93022-750, Brazil; julian.grub@gmail.com
7 Department of Agricultural and Biosystems Engineering, University of Ilorin, PMB 1515, Ilorin 240103, Nigeria; adbash2008@gmail.com
8 Department of Agricultural Civil Engineering, Kyungpook National University, Daegu 41566, Republic of Korea
* Correspondence: msilva@cuc.edu.co (M.L.S.O.); alcindo.neckel@atitus.edu.br (A.N.)

check for updates

Citation: Oliveira, M.L.S.; Valença, G.O.; Pinto, D.; Moro, L.D.; Bodah, B.W.; de Vargas Mores, G.; Grub, J.; Adelodun, B.; Neckel, A. Hazardous Elements in Sediments Detected in Former Decommissioned Coal Mining Areas in Colombia: A Need for Environmental Recovery. *Sustainability* **2023**, *15*, 8361. https://doi.org/10.3390/su15108361

Academic Editor: Shibao Chen

Received: 22 April 2023
Revised: 13 May 2023
Accepted: 18 May 2023
Published: 22 May 2023

Copyright: © 2023 by the authors. Licensee MDPI, Basel, Switzerland. This article is an open access article distributed under the terms and conditions of the Creative Commons Attribution (CC BY) license (https://creativecommons.org/licenses/by/4.0/).

Abstract: This study demonstrates an investigation into nanomineralogical and geochemical evolution for the detection of hazardous elements from old, abandoned coal mining deposits capable of causing negative environmental impacts. The general objective of this study is to evaluate the number of nanoparticulate chemical elements in sediments collected during the years 2017 and 2022 from deactivated coal mining areas in the La Guajíra and Cesar regions of Colombia. Sediments were collected and analyzed from areas that experienced spontaneous coal combustion (SCC). The analysis consisted of traditional mineralogical analysis by X-ray diffraction and Raman spectroscopy, nanomineralogy by field emission scanning electron microscope-FE-SEM, and high-resolution transmission electron microscope-HR-TEM (energy dispersive X-ray microanalysis system-EDS). The analyzed sediment samples contained high proportions of amorphous materials containing the chemical elements As, Cl, Hg, Mo, Pb, Sb, and Se. This study emphasizes the need to implement environmental recovery projects at former, now abandoned coal extraction areas located in the investigated region, as they have negative effects on the environment and human health across large regions.

Keywords: rare carbon compounds; spontaneous coal combustion; multi-analytical approach; sustainable macroscale

1. Introduction

It is important to highlight the relevance of studies capable of identifying probable environmental impacts originating from former mineral coal extraction sites, arguably the largest of which is the leaching of hazardous elements off-site [1,2]. The subsidy of environmental recovery projects that will guarantee the sustainability of such sites is key to protecting ecosystems on territorial macroscales. Abundant spontaneous coal combustion (SCC) has been studied by scientists worldwide due to the exposure of hazardous elements and polycyclic aromatic hydrocarbons [3]. SCC occurs in all countries where there is mining,

transport, storage, use, and disposal of coal-derived waste [4,5]. In addition to economic losses derived from the consumption of coal during SCC, this phenomenon negatively impacts the environment and human health due to completely uncontrolled emissions of harmful gases and particles into the atmosphere and both soil and water contamination from the leaching of multiple organic, inorganic and organometallic contaminants [6,7].

Studies emphasize the proliferation of contaminants from coal mining activities worldwide, where there are concerns about the quality of the environment and human health based on the significant impacts of environmental pollution from coal mining activities. Coal mining is capable of generating negative environmental impacts, including air and water pollution and soil degradation, contributing toward climate change and reduced biodiversity [8–12]. Finkelman [8] and Golik et al. [9] warn of possible environmental damage that can be caused by dangerous elements (Example: arsenic (As), cadmium (Cd), copper (Cu), lead (Pb), iron (Fe), mercury (Hg), selenium (Se) and antimony (Sb)) present in the environment after the process of extraction and burning of mineral coal as well as the deposition of coal fly ash in the environment. Golik et al. [9], when investigating the exposure of individuals to hazardous elements in coal mining dust from open pit mines. Of particular concern was soil contamination by chemical elements of metallic origin, capable of spreading over large regions depending on the intensity of the localized winds. Rybak et al. [10] highlight the hazards produced by the accumulation of high loads of waste, both from the mining process and the deposition of coal fly ash. Despite the economic need for continuous mineral coal extraction, mineral coal wastes, especially ash remaining after the burning process, contain several minerals capable of negatively impacting the environment. Minerals such as pyrite may cause irreversible changes in sediments and may spread through marine and terrestrial ecosystems [9,10]. Furthermore, adverse effects on the health of the local population are of significant concern [10,11].

Neckel et al. [11] emphasized the existence of contamination by hazardous chemical elements (As, Cu, Pb, Fe, Se, and Sb) arising from the extraction and transport of mineral coal from mining areas to a Caribbean port region in Colombia, compromising the environmental sustainability of marine and terrestrial ecosystems, also posing a risk to human health, especially to the local population that depends on fishing for food. Nanoparticles containing chemical elements that are dangerous to the environment and human health have sizes ranging from 1 to 100 μm in coal fly ash deposited in the environment following burning [12].

Solutions do exist to mitigate coal's potentially harmful impact on the environment. According to Wang et al. [13] and Khayrutdinov et al. [14], the mineral coal beneficiation process must face the organic materials of associated minerals in the form of nanoparticles and ultrafine particles, thereby generating technologies allocated to cleaner coal through physical separation methods (by gravity, electrostatic separation or magnetic), or with the use of physical-chemical separation (by bubble flotation, or agglomeration containing the use of oil).

One can highlight the use of multi-analytic studies using FE-SEM, HR-TEM, Mossbauer spectroscopy, petrology, X-ray diffraction, Raman spectroscopy, and complex chemical characterization (e.g., ion-pair chromatography coupled to inductively coupled plasma-mass spectrometry and liquid chromatography/electrospray ionization/tandem mass spectrometry) of SCC and its associated environmental impacts as well as human health risks have been evaluated by many scientific groups around the world [15–17]. The number of studies that reassess the impacts of SCC over the years is reduced, through the resampling of previously sampled locations, enabling quantitative analysis of hazardous elements in coal mining areas with more accurate results and realistic attributes quantitatively assigned in the environment [18,19].

Mineral coal mining areas are the sources of nanoparticles and ultrafine particles containing toxic compounds [19–21]. When precipitated, these compounds form oxides, sulfides, carbonates, hydroxides, and chlorides during the leaching process. Leaching

primarily occurs in coal mine drainage areas that contain tailings. The contaminants introduced through this leaching are capable of traveling and contaminating large regions.

Volatile chemical elements such as Cl, Br, F, and Hg can easily be emitted into the atmosphere and/or adsorbed by SCC by-products (especially Al-Fe-organic compounds), which accumulate in sediments in the form of nanoparticles and ultrafine particles [21–23]. Mineral coal has a high ability to combine with other elements, of inorganic and mineral origin, due to the ability of coal to associate with organic structures (aqueous), semi-solid organics, and gases [24,25]. This justifies the need for research capable of identifying the chemical elements present in coal, especially in former mining areas, which can negatively compromise the environmental quality of ecosystems [25].

Mineralogical transformations on a manometric scale, due to the high accumulation capacity of hazardous elements in the chemical structure of mineral coal, it is possible to signal future measures that enhance the mitigation of the accumulation of hazardous elements originating from former mineral coal mining areas, many of which are now abandoned and in the open [23,25]. Thus, the authors emphasize that scientific knowledge is crucial in the development of public policies that will support effective projects for the remediation of closed and/or abandoned coal mines and the use and disposal of coal fly ash in order to preserve environmental quality and remediate areas degraded by mineral coal extraction activities [26–28].

The general objective of this study is to evaluate the number of nanoparticulate chemical elements in sediments collected in former coal mining areas in the region of La Guajíra and Cesar (Colombia) in 2017 and 2022 in order to generate more accurate data regarding possible environmental impacts. This study is justified by demonstrating the number of hazardous elements accumulated over time [19,20,25] that are present in the chemical structures of mineral coal in the form of nanoparticles and ultrafine particles.

2. Materials and Methods

2.1. Studied Areas

By volume, Colombia is the fourth largest coal mining country in the world. However, it uses less than 10% of all coal mined domestically. The remaining 90% of its coal is exported abroad [29,30]. Colombia's main coal mines are located in the Paleocene Cerrejón Formation, in close proximity to the La Guajíra region, and the Paleocene Los Cuervos Formation near Cesar and Norte de Santander. While both are productive mining operations, the geology and petrographic characteristics of the two areas differ significantly, with classifications of mineral coal from Colombia varying between bituminous and anthracite [31]. Bituminous mineral coal comes from sedimentary rock aggregated by bitumen, which allows for a liquid mixture of high viscosity and dark color. The carbon content of bituminous mineral coal ranges from 80% to 90% and has a calorific value that varies from 7000 to 8650 kcal [32,33]. Anthracite coal, by contrast, is present in the soil in a compact and solid form with a carbon content that can exceed 96% in its purest form. Anthracite coal contains small or zero proportions of bitumen [32,33]. Study sites utilized for this study consisted of abandoned piles of mineral coal waste in both regions, La Guajíra (A) and Cesar (B) (Figure 1A,B). Sediment sampling aimed at the quantitative identification of hazardous elements in proportions of nanoparticles and ultrafine particles was conducted at each study site. As each pile is abandoned and in the open, mineral coal waste with the waste pile interacts with clays and quartz along with lower concentrations of sulfides, carbonates, phosphates and organometallic compounds, allowing for the accumulation of hazardous elements in the environment and potentially causing harm to human health [34].

The area studied in the region of La Guajíra, Colombia (A) is located on the Homonymous Peninsula. The region covers a total area of 20,848 km^2, with an estimated 2022 population of 880,560 inhabitants [35]. La Guajíra borders the Caribbean Sea to the west and north. It borders Venezuela to the east, the Cesar region to the south, and is bordered on the southwest by Magdalena, one of the most populated areas of Colombia. Magdalena had an approximate population of 1342 million inhabitants in 2022 [35]. The temperature

in the La Guajíra region varies between a minimum of 0 °C and a maximum of 30 °C. It is characterized by having the driest climate in Colombia [35]. The main economic activities in the region consist of mineral coal mining, tourism activities related to the Caribbean Sea, agriculture (sugar cane, rice, sesame, sorghum, cassava, cotton, and tobacco), and the raising of livestock (goats) [35,36]. Sample site A consists of an abandoned open pit coal mine that was also utilized as a dumping area for coal fly ash. Mining activities and dumping stopped in 2015.

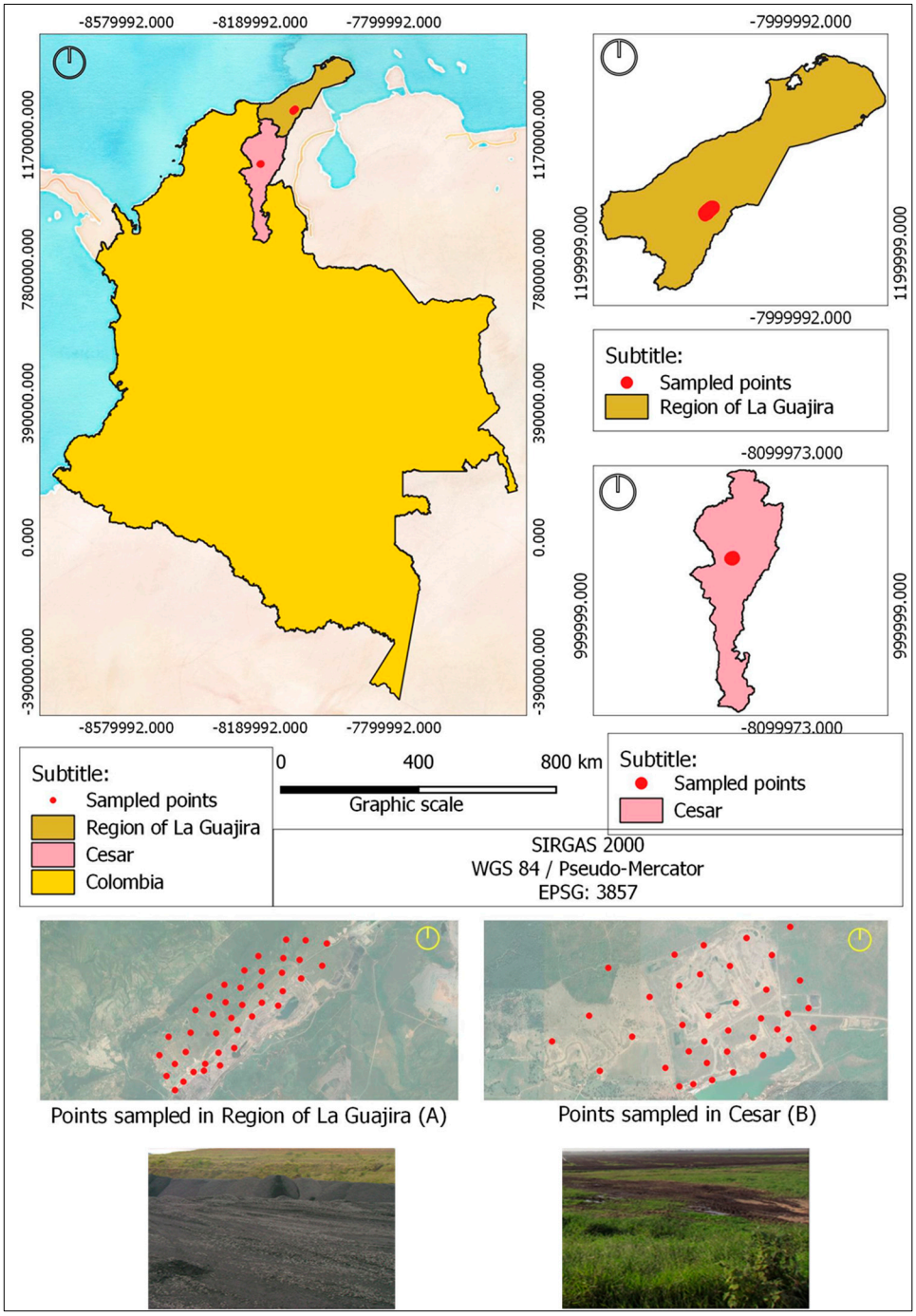

Figure 1. Location of the region of La Guajíra (**A**) and Cesar (**B**) in Colombia, photographs of the two sample sites, and map of sample locations within the two sites. Source: Adapted from the Subnational Administrative Boundaries database (Colombia), modeled in QGIS software, version 3.10.4, coupled with the Stamen Watercolor plugin.

Sample site B was located in the Cesar region of northeast Colombia. This region covers a territorial area of 22,905 km^2 and had an estimated population of 903,279 inhabitants in 2005. The Cesar region has a mixture of abandoned and active coal mines [35,37–39]. Sample site B was also located in an abandoned former mine utilized as a dump site for coal fly ash. Mining activities and dumping stopped in 2012. The Cesar region is bordered to the north by the regions of La Guajíra and Magdalena, to the south by the regions of Bolívar and Santander, and to the east by Venezuela [35]. The Cesar River flows through the Cesar region and serves as an important drinking water source for the region's capital, Valledupar. The river combines with the Ciénaga River in the city of Zapatosa, together forming the largest volume of fresh water in Colombia [35].

Neckel et al. [11], when studying the contamination resulting from dangerous elements present in Colombian coal, emphasize the concern around contamination of water resources. Contaminated water is capable of compromising the health of the population who consumes it, in addition to jeopardizing food subsistence over large regions. The food base of the population in this region is fishing. Annual temperatures fluctuate in the Cesar region between a maximum of 28 °C and a minimum of 4 °C [35].

2.2. Procedures Used in Sample Collection

Sample collection in the region of La Guajíra (A) and Cesar (B) (Figure 1) was carried out in summer between the months of February 2017 and 2022. Summer was chosen for sampling as this is the local dry season [35]. Sample collection was sanctioned by the Colombian government, which enables the proper collection of sediment samples from former abandoned coal mining areas.

Winter in the study area does not allow for the collection of sediments, as the sites remain flooded for the majority of the period between April and September due to intense precipitation. Overland flow in the area transports sediment to neighboring Colombian regions until it eventually flows into the Caribbean Sea [11,35].

Forty sediment samples were collected in the La Guajíra region (A), and forty sediment samples in Cesar (B) in 2017, and the same sediment collection procedure was repeated in 2022, using the same points sampled from 2017, totaling 160 sediment samples collected in total. The Global Positioning System (GPS) was used to mark the location of the points sampled from 2017 to 2022 by use of a Precision GPS (model L1 Magellan PromarK 3), with a maximum error of up to 40 cm. The marking of points by precision GPS is of fundamental importance, mainly in regions of difficult access. GPS enables researchers to generate greater reliability in research that involves the collection of sediments over time, as researchers can be assured they are sampling from the same location, which enables a historical series of sediment sampling [40].

The choice of the 40 points in each sampled location is due to the positioning of the construction of a Triangular Irregular Network (TIN), following the recommendation of the literature [41,42], in which it was determined that the spacing of the points in sediment collections should enhance a distance of 128 to 450 m from each sampled point, allowing greater reliability of studies, in relation to the number of points to be inserted in applied geospatial research.

The methodological recommendations of this study followed the procedure laid out by Dutta et al. [43], who specified that field collection of sediment samples are to be placed in sterilized glass containers, sealed and stored in Styrofoam thermal boxes, thereby preventing the possibility of contamination of the samples by external agents. Following collection, each sample was transported to the Barraquinhas Analytical Chemistry Laboratory at the Universidad de La Costa, CUC (Colombia) for analysis.

2.3. Analytical Methods

In the laboratory, all of the obtained SCC samples were dried in ovens with ventilation at 40 °C for 48 h to avoid the volatilization of volatile elements. The amount of each sample analytically processed weighed one kg. Samples were homogenized to form a

representative sample, as outlined in previous studies [44–46], in order to identify the number of chemical elements present. These representative samples, after being homogenized, were divided into three replicates, with three levels of replications (K3), totaling 480 test specimens for all samples collected in 2017 and 2022. This made it possible to demonstrate high reliability of the quantitative results of chemical elements identified in this study. Neckel et al. [11] and Dai et al. [47], when dealing with the identification of the presence of quantitative chemical elements in sediment samples in the laboratory for the quantitative identification of hazardous elements in certain regions, when the samples were homogenized, allowed for better identification of the types of chemical elements.

For Particle-Induced X-ray Emission (PIXE) and X-ray diffraction (XRD) (PANalytical X'Pert PRO-powder diffractometer-Malvern, UK) analyses, samples were ground to <212 μm and <100 μm to be analyzed by X-ray photoelectron spectroscopy (XPS), scanning electron microscopy (SEM), Raman Spectroscopy (RS) [48–50], inductively coupled plasma atomic emission spectrometry (ICP-AES) and inductively coupled plasma mass spectrometry (ICP-MS) [51,52] for trace chemical elements capable of evaluating the sample particles, considering the proportion of chemical elements in the samples collected [53,54]. The instrumental chemical analysis technique in ICP-AES allowed to stimulate the identification of chemical elements present in the sediments sampled in the region of La Guajíra (A) and Cesar (B), with the use of argon plasma at high temperatures of 7000–10,000 K, based on the form of fog generated at the center of the plasma [55]. As the atoms expand, they emit radiation which is then detected in wavelength by the analyzed elements in the range of 125 to 950 nm. The ICP-MS technique made it possible to carry out mass spectrometry on the samples collected in the region of La Guajíra (A) and Cesar (B), allowing for the detection of types of concentrated metals and non-metals on the sediments analyzed in certain isotopes [56]. This technique involves ionization, which, when coupled to plasma and a mass spectrometer, allows the separation and quantification of ions and is characterized as one of the most accurate techniques for identifying the types of chemical elements present in sediment samples [56,57].

The quantification of the chemical elements in the analyzed samples was carried out with the base structure of graphitic forms of fullerenes [58], with the objective of identifying the types of chemical elements in the samples. These methods evaluate neither the ultrafine/nanostructure nor the chemical configuration of ultrafine particles [59]. The authors' goal was to understand the structures of ultrafines and nanometrics that were studied in this work by HR-TEM, FE-SEM, and FIB-SEM, as all of these devices contain coupled EDS [53,54]. This study emphasizes that, for particles smaller than 50 nm, only the HR-TEM was robust, adapting better to the methodological procedure enough to understand the types of chemical elements present in the analyzed sediment samples, demonstrating a high degree of reliability in relation to the results obtained.

3. Results and Discussion

3.1. Characteristics Identified in the Analyzed Samples

Coal remaining at these sites is exposed to the open sky, consequently undergoing the natural processes of chemical, physical and biological weathering [60]. The action of wind and rain then transport the weathered material in the form of sediments over large regions, especially in times of great floods that frequently occur in the studied areas [35,37,60].

Fluvial dynamics, together with the weathering process, disaggregate coal particles with the potential to release chemical elements that are dangerous to human health and ecosystems over large regions, compromising the sustainability standards of local populations that depend on natural resources [61–63]. Although some authors use statistical methods to indirectly identify the mode of occurrence of elements [26,64], this study carries out the evaluation via HR-TEM and FE-SEM (both coupled with EDS). Using a detailed mineralogy of the most abundant minerals by XRD, Raman, and Mossbauer, the authors were able to identify the number of dangerous elements present in sediments with high accuracy [48,64,65].

Table 1 shows the minerals detected in the sediment samples collected in 2017 and 2022 from the regions of La Guajíra and Cesar. It is noted that, after the five-year sampling interval, several minerals, especially sulfate and sulfides, were no longer detected, while the proportion of amorphous materials increased. These data can be attributed to the intense action of weathering (a mixture of oxygen, water, microorganisms, and other factors) [62,63,66], which potentiates chemical reactions capable of quickly modifying some minerals that were initially identified in the sediment sampling carried out in 2017.

Table 1. Minerals detected in the La Guajía and Cesar regions, in 2017 and 2022.

Identified Elements	La Guajíra 2017	La Guajíra 2022	Cesar 2017	Cesar 2022
Fullerene s (C_{60}, C_{70}, C_{80})	▼	▲	▼	▲
Graphenes	▲	▲	▼	▲
Carbon nanotubes	▼	▲	▼	▲
Amorphous organic nanophases	▲	▲	▲	▲
Silicates				
Quartz, SiO_2	▲	▲	▲	▲
Chlorite, $Na_{0.5}Al_6(Si,Al)_8O_{20}(OH)_{10}.H_2O$	▲	▲	▲	▲
Illite, $K_{1.5}Al_4(Si_{6.5}Al_{1.5})O_{20}(OH)_4$	▲	▲	▲	▲
Kaolilite, $Al_2Si_2O_5(OH)_4$	▲	▲	▲	▲
Microcline, $KAlSi_3O_8$	▲	▲	▲	▲
Montmorillonite, $(Na,Ca)(Al,Mg)_2Si_4O_{10}(OH)_2.n(H_2O)$	▲	▲	▼	▲
Mullite, $Al_6Si_2O_{13}$	▲	▲	▼	▲
Muscovite, $KAl_2(AlSi_3)O_{10}(OH)_2$	▲	▲	▲	▲
Zircon, $ZrSiO_4$	▼	▼	▼	▼
Sulphides				
Bismuthinite, Bi_2S_3	▼	N.D.	N.D.	N.D.
Cattierite, CoS_2	▼	N.D.	N.D.	N.D.
Chalcopyrite, $CuFeS_2$	▼	N.D.	▼	▼
Galena, PbS	▼	N.D.	▼	N.D.
Marcasite, FeS_2	▼	N.D.	▼	N.D.
Molybdenite, MoS_2	▼	▼	▼	▼
Millerite, NiS	▼	▼	▼	▼
Pyrite, FeS_2	▼	▼	▼	▼
Pyrrhotite $Fe_{(1-x)}S$	▼	▼	▼	▼
Sphalerite, ZnS	▼	▼	▼	▼
Carbonates				
Calcite, $CaCO_3$	▼	N.D.	▼	N.D.
Dolomite, $CaMg(CO_3)_2$	▼	N.D.	▼	▼
Siderite, $FeCO_3$	▼	N.D.	▼	N.D.
Phosphates				
Brushite, $CaPO_3(OH).2H_2O$	▼	▼	▼	N.D.
Monazite, (Ce, La, Th, Nd, Y)PO_4	▼	▼	▼	▼
Xenotime, (Y, Er)PO_4	▼	▼	▼	▼
Sulfates				
Ammoniojarosite, $[(NH_4)Fe_3(SO_4)_2(OH)_6]$	▼	N.D.	▼	N.D.
Anhydrite, $CaSO_4$	▼	N.D.	▼	N.D.
Alunogen, $Al_2(SO_4)_3.17H_2O$	N.D.	N.D.	▼	▼
Barite, $BaSO_4$	▼	▼	▼	▼
Bassanite, $CaSO_4 \cdot 1/2H_2O$	N.D.	N.D.	N.D.	▼
Copiapite, $MgFe_4(SO_4)_6(OH_2)$ $18H_2O$	N.D.	N.D.	▼	N.D.
Coquimbite, $Fe_2(SO_4)_3 \cdot 9H_2O$	N.D.	N.D.	▼	N.D.
Epsomite, $MgSO_4$ $7H_2O$	N.D.	N.D.	N.D.	▼
Ferrohexahydrite, $FeSO_4$ $6H_2O$	N.D.	N.D.	N.D.	▼
Halotrichite, FeAl2 $(SO_4)_4.22H_2O$	N.D.	N.D.	N.D.	▼
Hexahydrite, $MgSO_4$ $6H_2O$	N.D.	N.D.	▼	▼
Gypsum, $Ca[SO_4] \cdot 2H_2O$	N.D.	N.D.	▼	▼

Table 1. *Cont.*

Identified Elements	La Guajíra 2017	La Guajíra 2022	Cesar 2017	Cesar 2022
Jarosite, $KFe^{3+}{}_3(SO_4)_2(OH)_6$	N.D.	N.D.	▼	▼
Melanterite, $FeSO_4\ 7H_2O$	N.D.	N.D.	▼	▼
Natrojarosite, $NaFe_3(SO_4)_2(OH)_6$	N.D.	N.D.	N.D.	N.D.
Pickeringite, $MgAl_2(SO_4)_4{\cdot}22H_2O$	N.D.	N.D.	▼	▼
Rozenite, $FeSO_4\ 4H_2O$	N.D.	N.D.	▼	N.D.
Schwertmannite, $Fe^{3+}{}_{16}O_{16}(OH)_{12}(SO_4)_2$	N.D.	N.D.	▼	N.D.
Oxides and hydroxides				
Anatase, TiO_2	▼	▼	▼	▼
Brookite, TiO_2	▼	▼	▼	▼
Chromite, $(Fe,Mg)Cr_2O_4$	▼	▼	▼	▼
Hematite, Fe_2O_3	▲	▲	▼	▲
Goethite, $Fe(OH)_3$	▼	▼	▼	▼
Gibbsite, $Al(OH)_3$	▼	▼	▼	▼
Maghemite, Fe_2O_3	▼	▼	▼	▼
Magnetite, Fe_3O_4	▼	▼	▼	▼
Rutile, TiO_2	▼	▼	▼	▼
Amorphous inorganic phases	▲	▲	▲	▲

▲More than 5%/▼minor proportion/N.D. = not detected.

Some mineral carbonates (e.g., calcite, dolomite, and siderite) were easily detected in the sediments sampled in 2017 in almost all analyzed samples. However, the sediments collected in 2022 at the same locations did not contain such minerals (Table 1). It was unexpected that dolomite was replaced or dissolved so easily in the environment. Normally, when carbonated, especially when rich in Mg, many years are needed to see such results unless there are sudden changes in environmental temperature and/or pressure [67,68]. Such minerals can generate both Ca-sulfates and amorphous phases widely detected in this study. This indicates a sequence of mineralogical formation [11,66] in which carbonates slowly degrade, forming sulfates and, subsequently, some amorphous phases. In some cases, this generates minerals such as mullite and montmorillonite. It was observed that, in the Cesar region, were observed 10% in abundance in the samples collected in 2017 but had increased to more than 20% in most of the sediment samples obtained five years later in 2022.

Phosphates are stable under high-temperature variations in the environment [69,70], but with these variations, the grains of these minerals can rupture or break, generating ultrafine particles and nanoparticles that are difficult to detect by FE-SEM [71–73]. However, when using FIB-SEM/EDS to prepare samples of sediments collected in the field, there was no difficulty in verifying minerals of great economic importance, such as monazine and xenotime, which are widely present in the regions. It should be noted that several REYs were also present in amorphous phases, which indicates that they are not present in the coals of the studied regions, but only as minerals associated with organic matter. Figure 2 illustrates the occurrence of REYs identified in amorphous phases.

Despite not being an abundant group of minerals, sulfates deserve great environmental relevance as Fe/Al sulfates can contain several dangerous elements aggregated in sediments [74–76]. In La Guajíra, lower proportions of sulfates were detected than in Cesar, where concentrations of sulfates were detected in greater proportions (Table 1). This demonstrates that, in the Cesar area, there is more precipitation and humidity than in the La Guajíra region [35], which facilitates the formation, mainly of hydrated sulfates (e.g., student, bassanite and copiapita) associated with the existence of coal tailings deposited in the open in the environment [77].

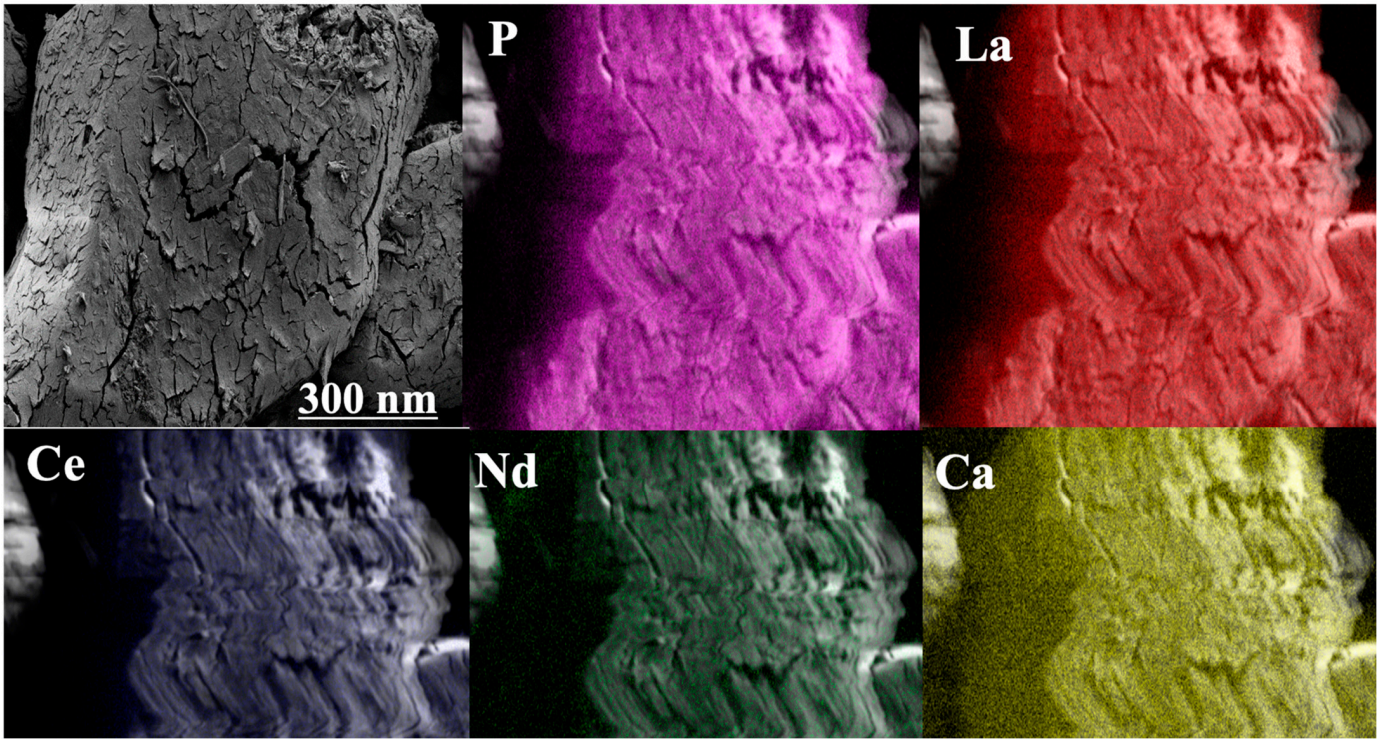

Figure 2. Amorphous particle containing REYs and Ca, widely detected in almost all samples after their preparation with FIB-SEM/EDS.

In this study, several complex mixtures containing the amorphous compounds melanterite and rozenite (Figure 3) were widely detected in the Cesar region. Another set of complex blends were between jarosite + natrojarosite (Figure 4), copiapite: Fe_2 + $Fe_{3+4}(SO_4)6(OH)_2 \cdot 20H_2O$. Mica, a generic term, refers to any of a group of approximately 30 silicate minerals occurring as non-fibrous plates. Muscovite (hydrated aluminum potassium silicate [$KA_{l2}(AlSi_3O_{10})(F, OH)_2$]). Micas are commonly found in ordinary rocks. In both sets of blends, we observed that some Fe-hydroxides and Fe-oxides were detected not in the same grains but around the sulfates, stimulated by the presence of coal tailings abandoned at the site after mining and the beneficiation process [77,78]. Similar results have been obtained previously with analyses of sediments conducted in other coal mining areas in several countries [77–79]. In this study, the main chemical elements, such as Si, Al, Fe, K, Mg, K, and P, coincide with the concentrations of the most abundant minerals (clays, carbonates, sulfides, and quartz). Both FE-SEM and HR-TEM work under a high vacuum. Therefore, many minerals can be identified using tools such as SEM + SAED + FFT. However, it is not always possible to obtain a photo as the samples may have destroyed minerals, especially sulfates, and hydroxides. Several particles from Figures 3 and 4 were sampled using FIB-SEM so that they could be later analyzed by HR-TEM/EDS/SAED, thus confirming the presence of several minor phases such as amorphous materials (containing Al and Si) as well as ammoniojarosite and natrojarosite. Without such a procedure, it would not be possible to detect such phases using only FE-SEM/EDS. After all, it is necessary to study the crystalline structure of minerals present on a nanometer scale, and this is only possible using equipment coupled with HR-TEM. It should be noted that even some sulfates can be perfectly analyzed and confirmed. However, the majority of the time, phases such as sulfates cannot be photographed as they are destroyed by the high vacuum required to operate the HR-TEM.

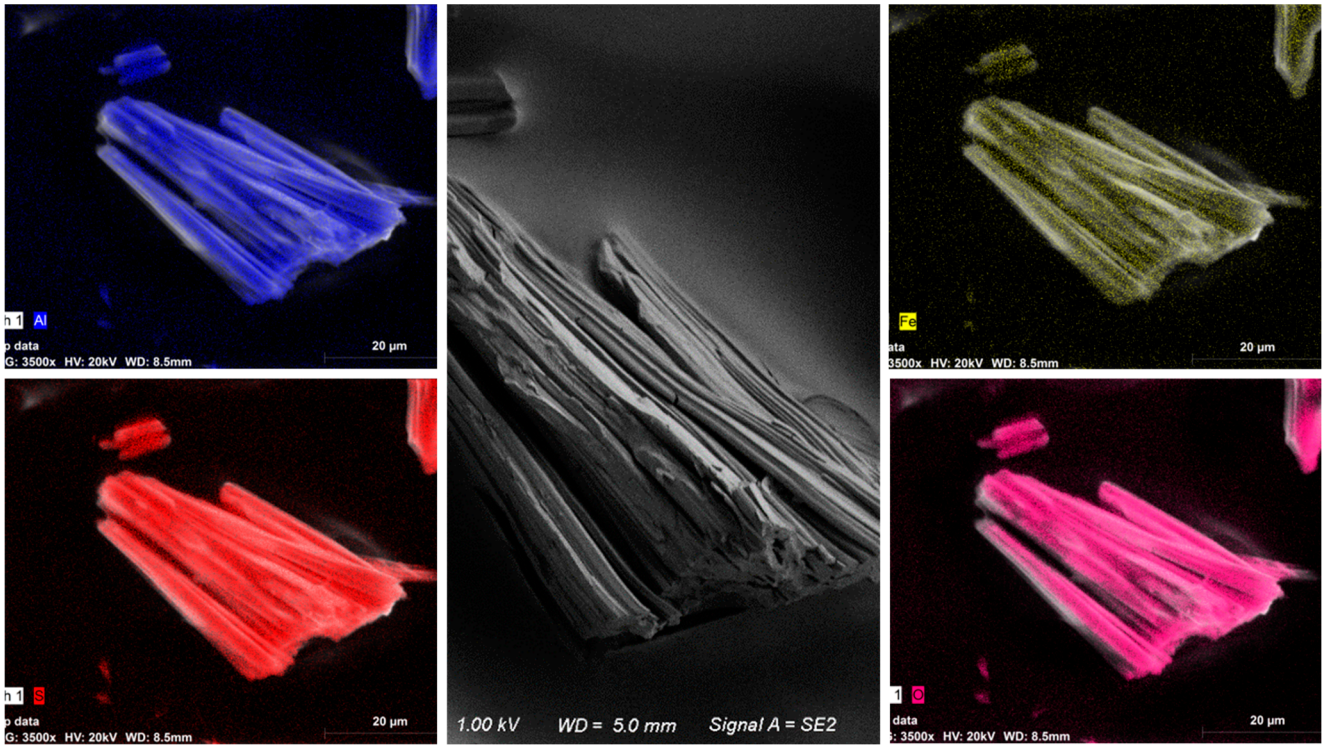

Figure 3. Typical complete mix between some sulfates, detected especially in the Cesar region.

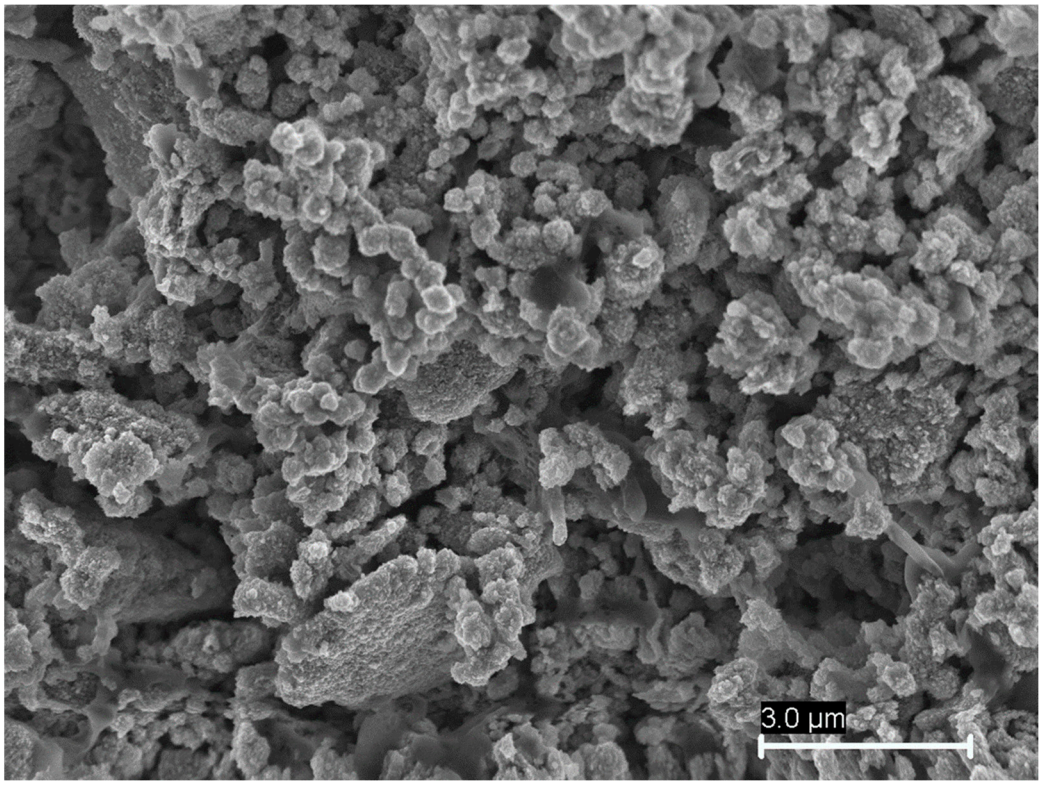

Figure 4. Clusters of jarosite, Ca-Fe-S-K-Al-amorphous phases, gypsum, ammoniojarosite and natrojarosite. Mineralogical evolutions such as this have been widely detected in the Cesar region.

The most volatile elements, such as halogens (Cl, Br, and F) and Hg, which were detected in 2017, were not detected in 2022 in the sediments collected in the La Guajíra region. However, Hg was detected in the Cesar region (Table 2). This is probably due to

the fact that they are more frequently associated with amorphous organometallic phases present in coal mining areas, more concentrated with greater amounts of C. Considering the sediments sampled in this study, it is likely that these chemical elements may be released into the atmosphere due to SCC. According to Ayaz et al. [7], SCC increases the probability of an abandoned mine contaminating large regions with elements that are dangerous to human health in addition to degrading the quality of local ecosystems. In the Cesar region, in addition to halogens, the elements As, Mo, Pb, Sb, Sn, and Zn were detected as sulfides or associated with sulfides, in addition to being present as Al-Si-amorphous phases. The explanation lies in the mineralogical transformation of sulfides in the presence of oxygen and humidity [77]. Rainfall rates in the region of La Guajíra and Cesar, according to official meteorological data from the Colombian government, resulted in less leaching associated with sulfides [35] during the period that the sediments were collected.

Table 2. Volatile and hazardous elements detected in analyzed sediments collected in 2017 and 2022.

Regions Studied	Elements
La Guajíra—2017	As, Be, Br, Cl, Cd, Co, Cu, Cr, F, Hg, La, Mn, Mo, Nb, Nd, Ni, Pb, S, Sb, Se, Sn, V, Y, Zn
La Guajíra—2022	As, Cd, Co, Cu, Cr, La, Mn, Mo, Nb, Nd, Ni, Pb, S, Sb, Se, Sn, V, Y, Zn
Cesar—2017	As, Be, Cl, Cd, Co, Cu, Cr, F, Hg, La, Mn, Mo, Nb, Nd, Ni, Pb, S, Sb, Se, Sn, V, Y, Zn
Cesar—2022	Cd, Co, Cu, Cr, Hg, La, Mn, Nb, Nd, Ni, Pb, S, Se, V, Y, Zn

Elements such as arsenic, cadmium, cobalt, lead, tin, antimony, and zinc decreased their concentrations considerably (up to 60%) when compared to the data reported by Neckel et al. [11]. This fact is certainly due to the partial volatilization of such chemical elements with the variation of ambient temperatures, generating a greater intensity of SCC in coal mining areas [77]. Yuan et al. [80] performed controlled tests for such elements and confirmed that almost all of them volatilize at low to intermediate temperatures, with the exception of Co, which is rarely vaporized. This depends on the combustion conditions and the type of coal where SCC occurs [80]. Yuan et al. [80] and Li et al. [81] have shown that antimony can volatilize at low temperatures (below 300 °C). Cd, Pb, Sn, and As volatilize at temperatures below 650 °C. Zinc volatilizes at temperatures below 950 °C, and Co volatilizes at temperatures below 1500 °C. These data can be used to interpret that the temperatures of the studied SCC may have exceeded 1500 °C, which has also been identified in other studies related to mineral coal [82–86]

The Cesar region has an average concentration of elements higher than the average concentration at La Guajíra, with little variation in both 2017 and 2022 (less than 15%) (Tables 3 and 4). It is noteworthy that some results were very similar in both years of study (2017 and 2022), being greater than 90% similar, which presented the most significant results in Tables 3 and 4. Although the areas sampled in the region of La Guajíra and Cesar are relatively close In geography, the chemical composition of the zones affected by SCC is not heterogeneous when compared to other localized areas such as the USA, Brazil, Spain, Portugal, and other countries [4,5,87,88]. Elements of greater toxicity were found in higher concentrations in the Cesar region. These findings are concerning as this area experiences higher rates of natural rainfall, which increases the mobility of toxic elements via erosion/runoff, overland flow, water percolation, and oxidation [89,90]. In old coal mining areas, it is necessary to implement projects with a high technological degree of environmental recovery that guarantee environmental sustainability; with the geomorphic remodeling of the degraded area, reconstruction of the soil and vegetation cover, hydrological stability with the direction of drainages, and contour lines, enabling ecological restoration in favor of the quality of hydrological and terrestrial ecosystems [89,91].

Table 3. Average, minimum and maximum compositions (% and ppm) in chemical elements homogenized and identified in samples collected from the La Guajíra region in 2017 and 2022.

Element	Mean	Min	Max
	(%)	(%)	(%)
Al	9.7	2.31	11.9
Ca	0.3	0.05	0.9
Fe	4.2	0.9	11.7
K	2.8	0.2	3.1
Mg	0.2	0.1	0.5
Na	0.3	0.1	0.5
Na	0.5	0.1	0.6
P	0.3	0.01	0.3
S	0.3	0.07	1
Ti	0.3	0.1	0.5
	(ppm)	(ppm)	(ppm)
As	37.8	19.2	108
Ba	501	132	843
Bi	0.5	0.3	0.9
Cd	0.3	0.1	0.6
Co	5.1	0.5	13.1
Cr	103	18.3	227
Cs	20.1	7.2	50.1
Cu	30.1	9.5	103.5
Ga	27.3	3.4	40.1
Li	153	9.1	303
Mn	119	7.3	1212
Mo	3.1	2.7	10.1
Nd	19.2	6.1	45.1
Ni	30.2	3.9	77.9
Pb	40.1	21.2	201
Sb	7.9	1.2	80.1
Sn	3.2	0.8	18.9
Sr	102	40.6	361
Ta	0.4	0.1	2.4
Th	19.6	8.6	20.3
U	3.1	1.1	6.8
V	101	42.5	191
W	3.9	0.9	8.1
Y	11.3	1.2	20.3
Zn	47.3	16.1	117
Zr	101	21.1	203

Table 4. Average, minimum and maximum compositions (% and ppm) in chemical elements homogenized and identified in samples collected from the Cesar region in 2017 and 2022.

Element	Mean	Min	Max
	(%)	(%)	(%)
Al	11.9	2.38	13.3
Ca	0.4	0.09	0.8
Fe	4.3	0.7	13.9
K	3.1	0.3	3.8
Mg	0.3	0.1	1.4
Na	0.4	0.1	0.9
Na	0.3	0.1	0.7
P	0.2	0.06	0.4
S	0.5	0.09	1.1
Ti	0.4	0.1	0.7

Table 4. *Cont.*

Element	Mean	Min	Max
	(ppm)	(ppm)	(ppm)
As	41.9	21.3	117
Ba	533	172	943
Bi	0.8	0.3	1.9
Cd	0.4	0.1	0.7
Co	6.8	0.9	18.5
Cr	133	21.2	292
Cs	23.1	8.2	58.2
Cu	38.4	12.7	122.2
Ga	30.7	4.4	44.7
Li	168	11.5	392
Mn	147	8.3	1811
Mo	4.7	3.3	13.9
Nd	20.3	7.1	49.8
Ni	33.8	4.9	80.7
Pb	43.1	19.2	299
Sb	9.8	1.9	81.3
Sn	4.5	0.9	21.3
Sr	111	47.1	347
Ta	1.4	0.8	6.3
Th	21.2	8.1	25.7
U	5.3	2	9.9
V	131	40.1	205
W	4.1	1.8	7.7
Y	14.9	6.8	28.1
Zn	51.2	17	141
Zr	118	23.1	219

When evaluating the difference between the samples collected in 2017 and 2022, it can be confirmed that the average chemical composition of the samples obtained shows a considerable increase. The concentration of some elements, such as REYs, increased by up to 17% due to the presence of halogens and Hg lost by volatilization.

3.2. Identification of Chemical Compounds with High-Added Value

Through Table 1, it is noted that fullerenes, graphenes, and carbon nanotubes show the same tendency to increase over the analyzed period. These data can be explained in the sense that SCC degrades the less stable phases of mineral coal but not the more stable phases, with structures more resistant to changes in ambient temperature. A similar argument was used to confirm the occurrence of similar phases in anthracite coals that probably experienced a temperature increase during their geological formation, which continued to occur steadily with ambient temperature [92,93].

Light REE (LREE) concentrations were between 159–381 ppm in samples from the La Guajíra region and between 189–427 ppm in samples from the Cesar region. In contrast, heavy REE (HREE) concentrations were between 124–297 in the La Guajíra region and between 139–329 ppm in the Cesar region. Large variations (above 25%) were not detected in terms of REY concentrations in the studied areas. Through Tables 1 and 2, it can be confirmed that some REYs tend to be more concentrated over time, which indicates that REYs naturally concentrate when degrading the organic phases present in mineral coal debris left in the open. Therefore, it is crucial that both REYs and carbon high-value phases (e.g., fullerenes and carbon nanotubes) so that not only are they detected, but their concentrations are better evaluated in the samples. Adequate detection methods must be developed regarding extractions from such phases. With this, environmental recovery projects can be developed with large monetary investments to aid in the recovery of environmental and societal impacts, not only in Colombia but worldwide.

Some inorganic elements present in the samples analyzed for this study pose a high potential risk for harm to human health and the environment [11]. However, several carboniferous elements and materials are also of high economic interest to the Colombian regions [94]. Given this scenario [77,94], the reuse of coal waste as a secondary source of raw material can be performed economically. This would not only prove to be a sustainable solution for the La Guajíra and Cesar regions but is necessary to provide adequate protection both for the environment and human health.

4. Conclusions

Achieving sustainability in and around abandoned coal mines is proving quite difficult. The degree of contamination in the environment and the possible risks to human health vary from site to site but are significant. Therefore, it is of fundamental importance to implement sustainable practices at these locations while they are in operation, in addition to dedicating resources toward the rehabilitation of former coal mining areas. Doing so contributes to the creation of a healthier environment, reduces the risk of accidents, and stimulates the local economy.

The abundant proportion of amorphous material composed especially of Al, Si, K, Fe, and Ca, in addition to several Fe oxides, indicates that over time the areas most affected by SCC become enriched with such phases. The different modes of occurrence of the amorphous phases observed in the SCC demonstrate that the combustion temperature reached in each study area was significantly heterogeneous. Considering our results, the chemical constitutions of the samples studied over the years show clear differences, most notably in areas more thermally affected by SCC. Potentially toxic elements were found in greater concentrations in the Cesar region as compared to La Guajíra. This is of concern when evaluating the risks to human health and the environment generated by SCC that favors the oxidation and percolation of water with the potential to remobilize chemical elements.

The significant reduction in the concentrations of halogens, Hg, As, Cd, Pb, Sb, Sn, and Zn, among other elements in the studied areas, is attributed to the partial and even total volatilization of these elements at high temperatures (between 400 °C and 1600 °C), confirming the mineralogical analysis and previous study on La Guajíra and Cesar.

The compounds and chemical elements significantly concentrated in the regions under study, REYs, and C-nanophases are considered critical raw materials globally, while other elements such as some halogens, mercury, arsenic, cobalt, copper, cadmium, lead, and uranium are environmentally sensitive and can have negative impacts on neighboring areas and human health. The reuse of materials present at former coal mining sites in both La Guajíra and Cesár as a secondary source of critical raw materials is probable, given the local economic reality. Therefore, funding projects to mitigate the environmental impacts caused by the deposition of coal tailings is of great importance. The present work, combined with the adequate comprehensive evaluation of areas in which SCC occurs, including the determination of the concentration of chemical elements and their modes of occurrence, contributes to the realization of future scientific studies dedicated to the extraction of compounds with the potential to harm the environment, in addition to being harmful to human health.

Author Contributions: Conceptualization, M.L.S.O., G.O.V., L.D.M. and D.P.; data curation, A.N.; formal analysis, J.G. and A.N.; funding acquisition, B.W.B.; investigation, L.D.M.; project administration, B.A. and D.P.; supervision, L.D.M. and G.d.V.M.; visualization, A.N.; writing—original draft preparation, M.L.S.O. and A.N.; writing—review and editing, B.A. and A.N. All authors have read and agreed to the published version of the manuscript.

Funding: This research received no external funding.

Institutional Review Board Statement: Not applicable.

Informed Consent Statement: Informed consent was obtained from all subjects involved in the study.

Data Availability Statement: Not applicable.

Acknowledgments: The authors are grateful to the Air Centre for supporting this research and the National Council for Scientific and Technological Development (CNPq) for the research productivity grant in Brazil. The authors also extend their thanks to the Center for Studies and Research on Urban Mobility (NEPMOUR+S/ATITUS), and Fundação Meridional, Brazil.

Conflicts of Interest: The authors declare no conflict of interest.

References

1. Wu, M.; Qi, C.; Chen, Q.; Liu, H. Evaluating the metal recovery potential of coal fly ash based on sequential extraction and machine learning. *Environ. Res.* **2013**, *224*, 115546. [CrossRef] [PubMed]
2. Sandeep, P.; Maity, S.; Mishra, S.; Chaudhary, D.K.; Dusane, C.; Pillai, A.S.; Kumar, A.V. Estimation of rare earth elements in Indian coal fly ashes for recovery feasibility as a secondary source. *J. Hazard. Mater.* **2023**, *10*, 100257. [CrossRef]
3. Tang, Y.; Hu, S.; Wang, H. Using P–Cl inorganic ultrafine aerosol particles to prevent spontaneous combustion of low-rank coal in an underground coal mine. *Fire Saf. J.* **2020**, *115*, 103140. [CrossRef]
4. Moghadam, M.J.; Ajalloeian, R.; Hajiannia, A. Preparation and application of alkali-activated materials based on waste glass and coal gangue: A review. *Constr. Build. Mater.* **2019**, *221*, 84–98. [CrossRef]
5. Dong, Z.; Ye, X.; Jiang, J.; Li, C. Life cycle assessment of coal-fired solar-assisted carbon capture power generation system integrated with organic Rankine cycle. *J. Clean. Prod.* **2022**, *356*, 131888. [CrossRef]
6. Li, Z.; Miao, Z.; Shen, X. Combined effects of water content and primary air volume on performance of lignite-fired boiler. *Fuel* **2019**, *244*, 580–591. [CrossRef]
7. Ayaz, M.; Jehan, N.; Nakonieczny, J.; Mentel, U.; Uz Zaman, Q. Health costs of environmental pollution faced by underground coal miners: Evidence from Balochistan, Pakistan. *Resour. Policy* **2022**, *76*, 102536. [CrossRef]
8. Finkelman, R.B. Potential health impacts of burning coal beds and waste banks. *Int. J. Coal Geol.* **2004**, *59*, 19–24. [CrossRef]
9. Golik, V.I.; Razorenov, I.I.; Vagin, V.S.; Liashenko, V.I. Study and development of hardening mixture composition based on unconventional industrial waste. Izvestiya Vysshikh Uchebnykh Zavedenii. *Gorn. Zh.* **2021**, *1*, 13–27. [CrossRef]
10. Rybak, J.; Gorbatyuk, S.M.; Bujanovna-Syuryun, K.C.; Khairutdinov, A.M.; Tyulyaeva, Y.S.; Makarov, P.S. Utilization of Mineral Waste: A Method for Expanding the Mineral Resource Base of a Mining and Smelting Company. *Metall.* **2021**, *64*, 851–861. [CrossRef]
11. Neckel, A.; Osorio-Martinez, J.; Pinto, D.; Bodah, B.W.; Adelodun, B.; Silva, L.F. Hazardous elements present in coal nanoparticles in a Caribbean port region in Colombia. *Sci. Total Environ.* **2022**, *838*, 156363. [CrossRef] [PubMed]
12. Zhang, W.; Wang, H.; Ma, Y.; You, C. Sulfur fixation for raw coal with combined microwave irradiation and ultrafine $Ca(OH)_2$ method. *Fuel* **2022**, *330*, 125570. [CrossRef]
13. Wang, G.; Bai, X.; Wu, C.; Li, W.; Liu, K.; Kiani, A. Recent advances in the beneficiation of ultrafine coal particles. *Fuel Process. Technol.* **2018**, *178*, 104–125. [CrossRef]
14. Khayrutdinov, M.M.; Golik, V.I.; Aleksakhin, A.V.; Trushina, E.V.; Lazareva, N.V.; Aleksakhina, Y.V. Proposal of an Algorithm for Choice of a Development System for Operational and Environmental Safety in Mining. *Resources* **2022**, *11*, 88. [CrossRef]
15. Neckel, A.; Pinto, D.; Adelodun, B.; Dotto, G.L. An Analysis of Nanoparticles Derived from Coal Fly Ash Incorporated into Concrete. *Sustainability* **2022**, *14*, 3943. [CrossRef]
16. Zhao, Y.; Zhang, J.; Chou, C.L.; Li, Y.; Wang, Z.; Ge, Y.; Zheng, C. Trace element emissions from spontaneous combustion of gob piles in coal mines, Shanxi, China. *Int. J. Coal Geol.* **2008**, *73*, 52–62. [CrossRef]
17. Ciesielczuk, J.; Misz-Kennan, M.; Hower, J.C.; Fabiańska, M.J. Mineralogy and geochemistry of coal wastes from the Starzykowiec coal-waste dump (Upper Silesia, Poland). *Int. J. Coal Geol.* **2014**, *127*, 42–55. [CrossRef]
18. Silva, L.F.; Pinto, D.; Dotto, G.L. A tool for realistic study of nanoparticulate coal rejects. *J. Clean. Prod.* **2021**, *278*, 121916. [CrossRef]
19. Yuan, B.; Cao, H.; Du, P.; Ren, J.; Chen, J.; Zhang, H.; Zhang, Y.; Luo, H. Source-oriented probabilistic health risk assessment of soil potentially toxic elements in a typical mining city. *J. Hazard. Mater.* **2023**, *443*, 130222. [CrossRef]
20. Padhye, L.P.; Jasemizad, T.; Bolan, S.; Tsyusko, O.V.; Unrine, J.M.; Biswal, B.K.; Balasubramanian, R.; Zhang, Y.; Zhang, T.; Zhao, J.; et al. Silver contamination and its toxicity and risk management in terrestrial and aquatic ecosystems. *Sci. Total Environ.* **2023**, *871*, 161926. [CrossRef]
21. Tretyakova, M.; Vardavas, A.; Vardavas, C.; Iatrou, E.; Stivaktakis, P.; Burykina, T.; Mezhuev, Y.; Tsatsakis, A.; Golokhvast, K. Effects of coal microparticles on marine organisms: A review. *Toxicol. Rep.* **2021**, *8*, 1207–1219. [CrossRef] [PubMed]
22. Onifade, M.; Genc, B. A review of research on spontaneous combustion of coal. *Int. J. Min. Sci. Technol.* **2020**, *30*, 303–311. [CrossRef]
23. Neckel, A.; Oliveira, M.L.; Castro Bolaño, L.J.; Maculan, L.S.; Moro, L.D.; Bodah, E.T.; Moreno-Ríos, A.L.; Bodah, B.W.; Silva, L.F. Biophysical matter in a marine estuary identified by the Sentinel-3B OLCI satellite and the presence of terrestrial iron (Fe) nanoparticles. *Mar. Pollut. Bull.* **2021**, *173*, 112925. [CrossRef]
24. Hower, J.C.; Finkelman, R.B.; Eble, C.F.; Arnold, B.J. Understanding coal quality and the critical importance of comprehensive coal analyses. *Int. J. Coal Geol.* **2022**, *263*, 104120. [CrossRef]

25. Hodson, M.E.; Islam, M.; Metcalf, M.; Wright, A.C. Amendments of waste ochre from former coal mines can potentially be used to increase soil carbon persistence. *Appl. Geochem.* **2023**, *151*, 105618. [CrossRef]
26. Dai, S.; Finkelman, R.B. Coal as a promising source of critical elements: Progress and future prospects. *Int. J. Coal Geol.* **2018**, *186*, 155–164. [CrossRef]
27. Harris, P.; McManus, P.; Sainsbury, P.; Viliani, F.; Riley, E. The institutional dynamics behind limited human health considerations in environmental assessments of coal mining projects in New South Wales, Australia. *Environ. Impact Assess. Rev.* **2021**, *86*, 106473. [CrossRef]
28. Hossen, M.A.; Chowdhury, A.I.H.; Mullick, M.R.A.; Hoque, A. Heavy metal pollution status and health risk assessment vicinity to Barapukuria coal mine area of Bangladesh. *Nanotechnol. Monit. Manag.* **2021**, *16*, 100469. [CrossRef]
29. Cardoso, A.; Turhan, E. Examining new geographies of coal: Dissenting energyscapes in Colombia and Turkey. *Appl. Energy* **2018**, *224*, 398–408. [CrossRef]
30. Huang, Q.; Talan, D.; Restrepo, J.H.; Baena, O.J.R.; Kecojevic, V.; Noble, A. Characterization study of rare earths, yttrium, and scandium from various Colombian coal samples and non-coal lithologies. *Int. J. Coal Geol.* **2019**, *209*, 14–26. [CrossRef]
31. López, I.C.; Ward, C.R. Composition and mode of occurrence of mineral matter in some Colombian coals. *Int. J. Coal Geol.* **2008**, *73*, 3–18. [CrossRef]
32. Blandón, A.; Gorin, G. Combining palynofacies and petrography in the study of sub-bituminous tropical coals: A case history from Lower Tertiary coals in Colombia. *Int. J. Coal Geol.* **2013**, *108*, 65–82. [CrossRef]
33. Moore, T.A.; Dai, S.; Huguet, C.; Pearse, J.; Liu, J.; Esterle, J.S.; Jia, R. Petrographic and geochemical characteristics of selected coal seams from the Late Cretaceous-Paleocene Guaduas Formation, Eastern Cordillera Basin, Colombia. *Int. J. Coal Geol.* **2022**, *259*, 104042. [CrossRef]
34. Silva, L.F.; Crissien, T.J.; Sampaio, C.H.; Hower, J.C.; Dai, S. Occurrence of carbon nanotubes and implication for the siting of elements in selected anthracites. *Fuel* **2020**, *263*, 116740. [CrossRef]
35. Dane. National Administrative Department of Statistics. Results National Census of Población of Vivienda. Santa Marta, Magdalena. 2019; pp. 1–46. Available online: https://www.dane.gov.co/files/censo2018/informacion-tecnica/presentaciones-territorio/191004-CNPV-presentacion-Magdalena.pdf (accessed on 28 January 2023).
36. Patricia, G.R.O.; Blandón, A.; Perea, C.; Mastalerz, M. Petrographic characterization, variations in chemistry, and paleoenvironmental interpretation of Colombian coals. *Int. J. Coal Geol.* **2020**, *227*, 103516. [CrossRef]
37. Akinyemi, S.A.; Bohórquez, F.; Islam, N.; Saikia, B.K.; Sampaio, C.H.; Crissien, T.J.; Silva, L.F. Petrography and geochemistry of exported Colombian coals: Implications from correlation and regression analyses. *Energy Geosci.* **2021**, *2*, 201–210. [CrossRef]
38. Hdx. Subnational Administrative Boundaries. This dataset is part of the Colombia. Data Grid Colombia. 2023. Available online: https://data.humdata.org/dataset/cod-ab-col? (accessed on 18 January 2023).
39. Qgis. Development Team. QGIS Geographic Information System. Open Source Geospatial Foundation Project. 2023. Available online: http://qgis.osgeo.org (accessed on 10 January 2023).
40. Higgitt, D.L.; Warburton, J. Applications of differential GPS in upland fluvial geomorphology. *Geomorphology* **1999**, *29*, 121–134. [CrossRef]
41. Luedeling, E.; Siebert, S.; Buerkert, A. Filling the voids in the SRTM elevation model-A TIN-based delta surface approach. *ISPRS J. Photogramm. Remote Sens.* **2007**, *62*, 283–294. [CrossRef]
42. Zhao, X.; Guo, Q.; Su, Y.; Xue, B. Improved progressive TIN densification filtering algorithm for airborne LiDAR data in forested areas. *ISPRS J. Photogramm. Remote Sens.* **2016**, *117*, 79–91. [CrossRef]
43. Dutta, M.; Saikia, J.; Taffarel, S.R.; Waanders, F.B.; Medeiros, D.d.; Cutruneo, C.M.; Silva, L.F.; Saikia, B.K. Environmental assessment and nano-mineralogical characterization of coal, overburden and sediment from Indian coal mining acid drainage. *Geosci. Front.* **2017**, *8*, 1285–1297. [CrossRef]
44. Silva, L.F.O.; Izquierdo, M.; Querol, X.; Finkelman, R.B.; Oliveira, M.L.S.; Wollenschlager, M.; Towler, M.; Pérez-López, R.; Macias, F. Leaching of potential hazardous elements of coal cleaning rejects. *Environ. Monit. Assess.* **2010**, *175*, 109–126. [CrossRef] [PubMed]
45. Ramsey, A.B.; Faiia, A.M.; Szynkiewicz, A. Eight years after the coal ash spill—Fate of trace metals in the contaminated river sediments near Kingston, eastern Tennessee. *Appl. Geochem.* **2019**, *104*, 158–167. [CrossRef]
46. Timpano, A.J.; Taylor, Z.; Jones, J.W. Contaminated interstitial sediment is a reservoir of trace elements with exposure potential for freshwater mussels. *Environ. Adv.* **2023**, *12*, 100357. [CrossRef]
47. Dai, S.; Finkelman, R.B.; French, D.; Hower, J.C.; Graham, I.T.; Zhao, F. Modes of occurrence of elements in coal: A critical evaluation. *Earth-Sci. Rev.* **2021**, *222*, 103815. [CrossRef]
48. Oliveira, M.L.; Pinto, D.; Tutikian, B.F.; Boit, K.d.; Saikia, B.K.; Silva, L.F. Pollution from uncontrolled coal fires: Continuous gaseous emissions and nanoparticles from coal mines. *J. Clean. Prod.* **2019**, *215*, 1140–1148. [CrossRef]
49. Li, K.; Liu, Q.; Hou, D.; Wang, Z.; Zhang, S. Quantitative investigation on the structural characteristics and evolution of high-rank coals from Xinhua, Hunan Province, China. *Fuel* **2021**, *289*, 119945. [CrossRef]
50. Sime, F.M.; Jin, J.; Wang, X.; Wick, C.D.; Miller, J.D. Characterization and simulation of graphite edge surfaces for the analysis of carbonaceous material separation from sulfide ores by flotation. *Miner. Eng.* **2022**, *182*, 107590. [CrossRef]

51. Rehan, I.; Gondal, M.; Almessiere, M.; Dakheel, R.; Rehan, K.; Sultana, S.; Dastageer, M. Nutritional and toxic elemental analysis of dry fruits using laser induced breakdown spectroscopy (LIBS) and inductively coupled plasma atomic emission spectrometry (ICP-AES). *Saudi J. Biol. Sci.* **2021**, *28*, 408–416. [CrossRef]
52. Galhardi, J.A.; García-Tenorio, R.; Bonotto, D.M.; Díaz Francés, I.; Motta, J.G. Natural radionuclides in plants, soils and sediments affected by U-rich coal mining activities in Brazil. *J. Environ. Radioact.* **2017**, *177*, 37–47. [CrossRef]
53. Montross, S.N.; Verba, C.A.; Chan, H.L.; Lopano, C. Advanced characterization of rare earth element minerals in coal utilization byproducts using multimodal image analysis. *Int. J. Coal Geol.* **2018**, *195*, 362–372. [CrossRef]
54. Kwiecińska, B.; Pusz, S.; Valentine, B.J. Application of electron microscopy TEM and SEM for analysis of coals, organic-rich shales and carbonaceous matter. *Int. J. Coal Geol.* **2019**, *211*, 103203. [CrossRef]
55. Roelandts, I.; Deblond, A. Rare-earth element composition of Devonian sediments from southern Belgium: Application of an inductively coupled plasma-atomic emission spectrometry method. *Chem. Geol.* **1992**, *95*, 167–176. [CrossRef]
56. Wei, W.J.; Yang, Y.; Li, X.Y.; Huang, P.; Wang, Q.; Yang, P.J. Cloud point extraction (CPE) combined with single particle-inductively coupled plasma-mass spectrometry (SP-ICP-MS) to analyze and characterize nano-silver sulfide in water environment. *Talanta* **2022**, *239*, 123117. [CrossRef] [PubMed]
57. Xiong, K.; Bu, W.; Ni, Y.; Liu, X.; Zheng, J.; Aono, T.; Yang, C.; Hu, S. Rapid monitoring of 241Am in small amount of sediment samples by combining extraction chromatography for highly efficient separation of interfering and matrix elements and ICP-MS/MS measurement. *Microchem. J.* **2023**, *190*, 108581. [CrossRef]
58. Sanchís, J.; Božović, D.; Al-Harbi, N.A.; Farré, M.; Barceló, D. Quantitative trace analysis of fullerenes in river sediment from Spain and soils from Saudi Arabia. *Anal. Bioanal. Chem.* **2013**, *405*, 5915–5923. [CrossRef]
59. Farag, S.; Konyashin, I.; Ries, B. The influence of grain growth inhibitors on the microstructure and properties of submicron, ultrafine and nano-structured hardmetals—A review. *Int. J Refract. Hard. Met.* **2018**, *77*, 12–30. [CrossRef]
60. Pandey, B.; Mukherjee, A.; Agrawal, M.; Singh, S. Assessment of Seasonal and Site-Specific Variations in Soil Physical, Chemical and Biological Properties Around Opencast Coal Mines. *Pedosphere* **2019**, *29*, 642–655. [CrossRef]
61. Tang, Q.; Sheng, W.; Li, L.; Zheng, L.; Miao, C.; Sun, R. Alteration behavior of mineral structure and hazardous elements during combustion of coal from a power plant at Huainan, Anhui, China. *Environ. Pollut.* **2018**, *239*, 768–776. [CrossRef]
62. Park, H.; Wang, L.; Yun, J.H. Coal beneficiation technology to reduce hazardous heavy metals in fly ash. *J. Hazard. Mater.* **2021**, *416*, 125853. [CrossRef]
63. Han, J.; Yu, D.; Wang, Q.; Yu, N.; Wu, J.; Liu, Y.; Luo, L.; Pan, H. Beneficiation of coal ash from ash silos of six Chinese power plants and its risk assessment of hazardous elements for land application. *Process Saf. Environ. Prot.* **2022**, *160*, 641–649. [CrossRef]
64. Eskanazy, G.; Finkelman, R.B.; Chattarjee, S. Some considerations concerning the use of correlation coefficients and cluster analysis in interpreting coal geochemistry data. *Int. J. Coal Geol.* **2010**, *83*, 491–493. [CrossRef]
65. Silva, L.F.; Crissien, T.J.; Schneider, I.L.; Blanco, R.P.; Sampaio, C.H. Nanometric particles of high economic value in coal fire region: Opportunities for social improvement. *J. Clean. Prod.* **2020**, *256*, 120480. [CrossRef]
66. Liu, Y.; Molinari, S.; Dalconi, M.C.; Valentini, L.; Ricci, G.; Carrer, C.; Ferrari, G.; Artioli, G. The leaching behaviors of lead, zinc, and sulfate in pyrite ash contaminated soil: Mineralogical assessments and environmental implications. *J. Environ. Chem. Eng.* **2023**, *11*, 109687. [CrossRef]
67. Salih, N.; Mansurbeg, H.; Muchez, P.; Axel, G.; Préat, A. Hydrothermal Fluids and Cold Meteoric Waters along Tectonic-Controlled Open Spaces in Upper Cretaceous Carbonate Rocks, NE-Iraq: Scanning Data from In Situ U-Pb Geochronology and Microthermometry. *Water* **2021**, *13*, 3559. [CrossRef]
68. Salih, N. The Impact of Hydrothermal Fluids on Porosity Enhancement and Hydrocarbon Migration in Qamchuqa Formation, Lower Cretaceous, Kirkuk Oil Company. *Minerals* **2023**, *13*, 377. [CrossRef]
69. He, X.; Wu, J.; Chen, Y.; Zhang, L.; Sheng, X. A trace amount of MXene@PDA nanosheets for low-temperature zinc phosphating coatings with superb corrosion resistance. *Appl. Surf. Sci.* **2022**, *603*, 154455. [CrossRef]
70. Jiang, Z.; Nie, K.; Arinzechi, C.; Li, J.; Liao, Q.; Si, M.; Yang, Z.; Li, Q.; Yang, W. Cooperative effect of slow-release ferrous and phosphate for simultaneous stabilization of As, Cd and Pb in soil. *J. Hazard. Mater.* **2023**, *452*, 131232. [CrossRef]
71. Wang, Y.; Xie, X.; Chen, X.; Huang, C.; Yang, S. Biochar-loaded Ce^{3+}-enriched ultra-fine ceria nanoparticles for phosphate adsorption. *J. Hazard. Mater.* **2020**, *396*, 122626. [CrossRef]
72. Moumen, E.; Bazzi, L.; El Hankari, S. Metal-organic frameworks and their composites for the adsorption and sensing of phosphate. *Coord. Chem. Rev.* **2022**, *455*, 214376. [CrossRef]
73. Kamal, S.; Khalid, M.; Khan, M.S.; Shahid, M. Metal organic frameworks and their composites as effective tools for sensing environmental hazards: An up to date tale of mechanism, current trends and future prospects. *Coord. Chem. Rev.* **2023**, *474*, 214859. [CrossRef]
74. Ma, W.; Liu, S.; Li, Z.; Lv, J.; Yang, L. Release and transformation mechanisms of hazardous trace elements in the ash and slag during underground coal gasification. *Fuel* **2020**, *281*, 118774. [CrossRef]
75. Marove, C.A.; Tangviroon, P.; Tabelin, C.B.; Igarashi, T. Leaching of hazardous elements from Mozambican coal and coal ash. *J. Afr. Earth Sci.* **2020**, *168*, 103861. [CrossRef]
76. Ali, M.U.; Liu, Y.; Yousaf, B.; Wong, M.H.; Li, P.; Liu, G.; Wang, R.; Wei, Y.; Lu, M. Morphochemical investigation on the enrichment and transformation of hazardous elements in ash from waste incineration plants. *Sci. Total Environ.* **2022**, *828*, 154490. [CrossRef] [PubMed]

77. Lahrouch, F.; Baptiste, B.; Dardenne, K.; Rothe, J.; Elkaim, E.; Descostes, M.; Gerard, M. Uranium speciation control by uranyl sulfate and phosphate in tailings subject to a Sahelian climate, Cominak, Niger. *Chemosphere* **2022**, *287*, 132139. [CrossRef] [PubMed]
78. Wang, C.; Zhao, L.; Sun, R.; Hu, Y.; Tang, G.; Chen, W.; Du, Y.; Che, D. Effects of silicon-aluminum additives on ash mineralogy, morphology, and transformation of sodium, calcium, and iron during oxy-fuel combustion of zhundong high-alkali coal. *Int. J. Greenh. Gas Control.* **2019**, *91*, 102832. [CrossRef]
79. Arbuzov, S.; Chekryzhov, I.; Spears, D.; Ilenok, S.; Soktoev, B.; Popov, N. Geology, geochemistry, mineralogy and genesis of the Spetsugli high-germanium coal deposit in the Pavlovsk coalfield, Russian Far East. *Ore Geol. Rev.* **2021**, *139*, 104537. [CrossRef]
80. Yuan, Z.; Jia, G.; Cui, X.; Song, X.; Wang, C.; Zhao, P.; Ragauskas, A.J. Effects of temperature and time on supercritical methanol Co-Liquefaction of rice straw and linear low-density polyethylene wastes. *Energy* **2022**, *245*, 123315. [CrossRef]
81. Li, B.; Zhuang, X.; Querol, X.; Moreno, N.; Córdoba, P.; Shangguan, Y.; Yang, L.; Li, J.; Zhang, F. Geological controls on the distribution of REY-Zr (Hf)-Nb (Ta) enrichment horizons in late Permian coals from the Qiandongbei Coalfield, Guizhou Province, SW China. *Int. J. Coal Geol.* **2022**, *231*, 103604. [CrossRef]
82. Ribeiro, J.; Flores, D.; Ward, C.R.; Silva, L.F. Identification of nanominerals and nanoparticles in burning coal waste piles from Portugal. *Sci. Total Environ.* **2010**, *408*, 6032–6041. [CrossRef]
83. Silva, L.F.; Oliveira, M.L.; Neace, E.R.; O'Keefe, J.M.; Henke, K.R.; Hower, J.C. Nanominerals and ultrafine particles in sublimates from the Ruth Mullins coal fire, Perry County, Eastern Kentucky, USA. *Int. J. Coal Geol.* **2011**, *85*, 237–245. [CrossRef]
84. Silva, L.F.; Oliveira, M.L.; Philippi, V.; Serra, C.C.; Hower, J.C.; Xue, W.; Chen, W.; O'Keefe, J.M.; Romanek, C.S.; Hopps, S.D.; et al. Geochemistry of carbon nanotube assemblages in coal fire soot, Ruth Mullins fire, Perry County, Kentucky. *Int. J. Coal Geol.* **2012**, *94*, 206–213. [CrossRef]
85. Hower, J.C.; O'Keefe, J.M.; Henke, K.R.; Wagner, N.; Copley, G.C.; Blake, D.R.; Garrison, T.M.; Oliveira, M.L.; Kautzmann, R.M.; Silva, L.F. Gaseous emissions and sublimates from the Truman Shepherd coal fire, Floyd County, Kentucky: A re-investigation following attempted mitigation of the fire. *Int. J. Coal Geol.* **2013**, *116–117*, 63–74. [CrossRef]
86. Wilcox, J.; Wang, B.; Rupp, E.C.; Taggart, R.K.; Hsu-Kim, H.; Oliveira, M.L.; Cutruneo, C.M.; Taffarel, S.R.; Silva, L.F.; Hopps, S.D.; et al. Observations and Assessment of Fly Ashes from High-Sulfur Bituminous Coals and Blends of High-Sulfur Bituminous and Subbituminous Coals: Environmental Processes Recorded at the Macro-and Nanometer Scale. *Energy Fuels* **2015**, *29*, 7168–7177. [CrossRef]
87. George, A.; Shen, B.; Kang, D.; Yang, J.; Luo, J. Emission control strategies of hazardous trace elements from coal-fired power plants in China. *J. Environ. Sci.* **2020**, *93*, 66–90. [CrossRef] [PubMed]
88. Ribeiro, J.; Suárez-Ruiz, I.; Flores, D. Coal related fires in Portugal: New occurrences and new insights on the characterization of thermally affected and non-affected coal waste piles. *Int. J. Coal Geol.* **2022**, *252*, 103941. [CrossRef]
89. Feng, Y.; Wang, J.; Bai, Z.; Reading, L. Effects of surface coal mining and land reclamation on soil properties: A review. *Earth-Sci. Rev.* **2019**, *191*, 12–25. [CrossRef]
90. Lieberman, N.R.; Izquierdo, M.; Muñoz-Quirós, C.; Cohen, H.; Chenery, S.R. Geochemical signature of superhigh organic sulphur Raša coals and the mobility of toxic trace elements from combustion products and polluted soils near the Plomin coal-fired power station in Croatia. *Appl. Geochem.* **2020**, *114*, 104472. [CrossRef]
91. Xiong, X.; Liu, X.; Yu, I.K.; Wang, L.; Zhou, J.; Sun, X.; Rinklebe, J.; Shaheen, S.M.; Ok, Y.S.; Lin, Z.; et al. Potentially toxic elements in solid waste streams: Fate and management approaches. *Environ. Pollut.* **2019**, *253*, 680–707. [CrossRef]
92. Dill, H.G.; Jolanta, K.; Andrei, B.; Sorin-Ionut, B.; Stephan, K.; Borrego, A.G. Organic debris and allochthonous coal in Quaternary landforms within a periglacial setting (Longyearbyen Mining District, Norway)—A multi-disciplinary study (coal geology-geomorphology-sedimentology). *Int. J. Coal Geol.* **2021**, *233*, 103625. [CrossRef]
93. Zhang, B.; Shen, Z.; Sun, J.; Zou, H.; He, K.; Wang, X.; Li, J.; Cui, S.; Zhang, N.; Cao, J. Emission characteristics and formation mechanisms of $PM_{2.5}$ and gases from different geological maturities coals combustion. *Fuel* **2022**, *315*, 123240. [CrossRef]
94. Vo, T.L.; Nash, W.; Del Galdo, M.; Rezania, M.; Crane, R.; Mousavi Nezhad, M.; Ferrara, L. Coal mining wastes valorization as raw geomaterials in construction: A review with new perspectives. *J. Clean. Prod.* **2022**, *336*, 130213. [CrossRef]

Disclaimer/Publisher's Note: The statements, opinions and data contained in all publications are solely those of the individual author(s) and contributor(s) and not of MDPI and/or the editor(s). MDPI and/or the editor(s) disclaim responsibility for any injury to people or property resulting from any ideas, methods, instructions or products referred to in the content.